PCCP

Accepted Manuscript

ROYAL SOCIETY OF CHEMISTRY

www.rsc.org/pccp

Cite this: DOI: 10.1039/c0xx00000x

www.rsc.org/xxxxxx

ARTICLE TYPE

Tunable photoluminescence and magnetic properties of Dy^{3+} and Eu^{3+} doped $GdVO_4$ multifunctional phosphors

Yanxia Liu, Guixia Liu*, Xiangting Dong, Jinxian Wang and Wensheng Yu

Received (in XXX, XXX) Xth XXXXXXXXX 20XX, Accepted Xth XXXXXXXXX 20XX

DOI: 10.1039/b000000x

A series of Dy^{3+} or/and Eu^{3+} doped $GdVO_4$ phosphors were successfully prepared by a simple hydrothermal method and characterized by X-ray diffraction (XRD), field emission scanning electron microscope (FE-SEM), energy-dispersive X-ray spectrometer (EDS), photoluminescence (PL) spectra and vibrating sample magnetometer (VSM). The results indicate that the as-prepared samples are pure tetragonal phase $GdVO_4$, taking on nanoparticles with an average size of 45 nm. Under ultraviolet (UV) light excitation, the individual Dy^{3+} or Eu^{3+} ions activated $GdVO_4$ phosphors exhibit excellent emission properties in their respective regions. The mechanism of energy transfer from VO_4^{3-} group and charge transfer band (CTB) to Dy^{3+} and Eu^{3+} ions is proposed. Color-tunable emissions in $GdVO_4$: Dy^{3+}, Eu^{3+} phosphors are realized through adopting different excitation wavelengths or adjusting appropriate concentration of Dy^{3+} and Eu^{3+} when excited by a single excitation wavelength. In addition, the as-prepared samples show paramagnetic properties at room temperature. This kind of multifunctional color-tunable phosphors has great potential applications in the fields of photoelectronic devices and biomedical sciences.

1 Introduction

In recent years, considerable attention has been paid to design and preparation of rare-earth ions doped $GdVO_4$ luminescent materials due to their outstanding optical, electronic and magnetic properties[1,2]. Gd^{3+} ions can be easily replaced by other luminescence rare-earth ions because of the equal valence and similar ionic radii. Rare-earth ions doped $GdVO_4$ luminescent materials can emit the light with various colors because of the strong UV light absorption of the VO_4^{3-} group and CTB, and an efficient energy transfer from VO_4^{3-} group and CTB to activators. Moreover, since the Gd^{3+} ($4f^7$, $^8S_{7/2}$) ions with seven unpaired 4f electrons possess a large electron magnetic moment, rare-earth ions doped $GdVO_4$ materials can function as multifunctional materials which have potential applications in biomedicine. It should be noted that this kind of materials has been widely utilized in the fields of light emitting diodes (LEDs)[3,4], full-color displays[5,6], cell imaging[7,8] and fluorescent labels[9,10] due to their unique coupled behaviors.

It is well documented that Dy^{3+} ($4f^9$) ions doped materials mainly emit blue and yellow light due to the $^4F_{9/2}\rightarrow{}^6H_{15/2}$ transition (478 nm) and $^4F_{9/2}\rightarrow{}^6H_{15/2}$ transition (574 nm). Eu^{3+} ions are of great research interest for the excellent red emission originated from the $^5D_0\rightarrow{}^7F_2$ (about 620 nm) transition in the visible range. Thereby, multicolor photoluminescence including white light could be easily realized by co-doping Dy^{3+} and Eu^{3+} ions into a single-phase host. In recent years, tunable photoluminescence properties of the Dy^{3+} and Eu^{3+} ions have been widely studied in many hosts, such as Y_2O_2S: Eu^{3+}/Dy^{3+}[11], $ZnWO_4$: Eu^{3+}/Dy^{3+}[12], $Ca_2La_8(GeO_4)_6O_2$: Eu^{3+}/Dy^{3+}[13], $BaLa_2WO_7$: Eu^{3+}/Dy^{3+}[14] and Sr_3AlO_4F: Eu^{3+}/Dy^{3+}[15]. Based on the above researches and in consideration of the characteristic emissions of Dy^{3+} and Eu^{3+} ions, it is expected that multicolor emissions also could be achieved in $GdVO_4$ system by employing different Dy^{3+} and Eu^{3+} dopants for their abundant 4f-orbital electronic transitions. Up to now, most reports about $GdVO_4$ luminescent materials have mainly been focused on rare-earth ions singly activated $GdVO_4$ host in the literature[16-18]. In addition, multicolor materials have been reported widely based on fluorides[19,20], molybdates[21], phosphates[22], tungstate[23] and borates[24] doped with different activators combinations. However, there are a few reports about vanadate compared to the other hosts, moreover, vanadate host shows relatively excellent chemical and photophysical stability. Hence, it is highly valuable to obtain color-tunable emissions through doping Dy^{3+} along with Eu^{3+} into $GdVO_4$ host.

In this work, we report on the preparation, luminescence and magnetic properties of Dy^{3+} or/and Eu^{3+} doped $GdVO_4$ phosphors synthesized by a simple hydrothermal method. The photoluminescence properties of the samples were analyzed by excitation and emission spectra while the magnetic properties were characterized by a VSM. At the same time, multicolor photoluminescence have been realized in $GdVO_4$ system through two methods.

2 Experimental sections

2.1 Chemicals

Gd_2O_3, Dy_2O_3, Eu_2O_3 (99.99%) and orthovanadate dodecahydrate ($Na_3VO_4 \cdot 12H_2O$) were purchased from Sinopharm Chemical Reagent Co., Ltd. Sodium dodecyl sulfate ($C_{12}H_{25}SO_4Na$), HNO_3 were purchased from Xilong Chemical Co., Ltd. All of the chemicals were of analytical grade and utilized as purchased without any further purification.

2.2 Preparation

Aqueous solutions of $Gd(NO_3)_3$, $Dy(NO_3)_3$ and $Eu(NO_3)_3$ were achieved by dissolving the corresponding amount of rare earth oxides Gd_2O_3, Dy_2O_3, Eu_2O_3 in dilute HNO_3 solution under heating with agitation in ambient atmosphere. A series of rare earth ions doped $GdVO_4$ samples were prepared by a simple hydrothermal method. The typical procedure for preparation $GdVO_4$: $0.01Dy^{3+}$, 0.02 Eu^{3+} was as follows: 1.0 mmol of $RE(NO_3)_3$ mixed solution (including 0.97 mmol $Gd(NO_3)_3$, 0.01 mmol $Dy(NO_3)_3$ and 0.02 mmol $Eu(NO_3)_3$) was added into 100 mL flask containing 30 mL water. Then $Na_3VO_4 \cdot 12H_2O$ (1 mmol) was added into the above mixed solution with continuous stirring for 0.5 h, $C_{12}H_{25}SO_4Na$ (2 mmol) was introduced into the mixture subsequently and stirred for another 0.5 h, the well-stirred suspension was poured into a 50 mL Teflon-lined stainless steel autoclave and then treated for 24 h at 180 °C. After that, the autoclave was naturally cooled down to the room temperature. Finally, the as-prepared precipitates were separated by centrifugation at 10000 r/min for 3 min, washed with de-ionized water and ethanol for several times, and then dried in air at 60 °C for 12 h. The synthetic procedures of other samples were the same with $GdVO_4$: $0.01Dy^{3+}$, 0.02 Eu^{3+} samples except for using the corresponding proper amount of rare earth ions.

2.3 Characterization

Powder X-ray diffraction (XRD) patterns were performed on a X-ray diffractometer (Rigaku D/max-RA, Cu Kα, λ= 0.15406 nm), operating at a scanning speed of 10° min^{-1} in the 2θ range from 10° to 90°, 30 mA, 40 kV. The morphology and composition of the samples were analyzed with a FEI-30 field emission scanning electron microscope (FE-SEM) equipped with an energy-dispersive X-ray spectrometer (EDS). The photoluminescence spectra and lifetimes of the samples were obtained by a HITACHI F-7000 Fluorescence Spectrophotometer equipped with a 150 W xenon lamp as the excitation source. A VSM was employed to measure the magnetization of the as-prepared samples with the applied magnetic field ranging from -20 to 20 kOe. All of the measurements were performed at room temperature.

3 Results and discussion

3.1 Phase, structure and morphology

Fig. 1 (a) shows the XRD patterns of Dy^{3+} or/and Eu^{3+} doped $GdVO_4$ samples prepared by hydrothermal method at 180 °C for 24 h. It can be seen that all the peaks in the patterns match well with the characteristic reflections of pure $GdVO_4$ (JCPDS Card no.72-0277), which has a zircon type structure of tetragonal system with the I41/amd space group. No any other peaks can be observed, revealing that the samples were pure phase $GdVO_4$. In addition, compared with pure $GdVO_4$, one can see that the main peaks slightly shift towards to the higher degree by the introduction of Dy^{3+} ions, but for the doping of Eu^{3+} ions or Eu^{3+} and Dy^{3+} ions the main peaks shift slightly to lower degree. This is because that the ionic radii of the Gd^{3+} ions (0.938 Å) are larger than that of Dy^{3+} ions (0.912 Å) and smaller than that of Eu^{3+} ions (0.947 Å)[25]. Hence, the results imply that Dy^{3+} and Eu^{3+} ions are undoubtedly entered into the lattices of the $GdVO_4$ host without changing the crystalline structure of the samples. Fig. 1 (b) and (c) exhibit schematic presentation of $GdVO_4$ tetragonal structure. $GdVO_4$ crystal consists of VO_4 tetrahedron in which V^{5+} ions are tetrahedrally coordinated by O^{2-} ions and distorted GdO_8 dodecahedron (eightfold) in which Gd^{3+} ions are linked with eight neighboring O^{2-} ions. Along the c-axis, alternating dodecahedron and tetrahedron shares edges with Gd^{3+} and V^{5+} ions are in a direct line, while in a and b direction four adjacent VO_4 units are connected by corners with GdO_8 polyhedron. Among these four tetrahedrons, two locate along the direction [100] while the other two lie along the direction [010][26-29].

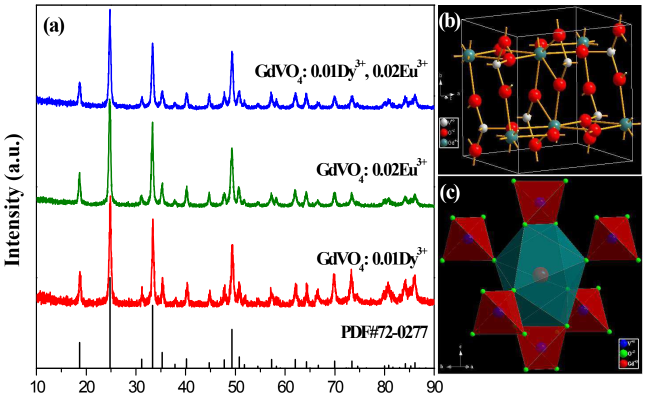

Fig. 1 (a) XRD patterns of the as-prepared $GdVO_4$: Dy^{3+}, $GdVO_4$: Eu^{3+} and $GdVO_4$: Dy^{3+}, Eu^{3+} samples, the corresponding standard data of $GdVO_4$ (JCPDS No.72-0277) is given as reference; (b) the crystal structure unit and (c) the coordination mode for tetragonal $GdVO_4$ crystals.

The morphology and composition of $GdVO_4$: $0.02Dy^{3+}$, $0.02Eu^{3+}$ samples are characterized by FE-SEM and EDS. As depicted in Fig. 2 (a), the as-prepared samples are composed of a large number of nanoparticles with a mean size of 45 nm, as the inset shown. Fig. 2 (b) presents the EDS spectrum of the products, which confirms the chemical composition of the samples, including O, V, Gd, Dy, Eu, Si and Cr (silicon and chromium signals arise from silicon host and spraying chromium process).

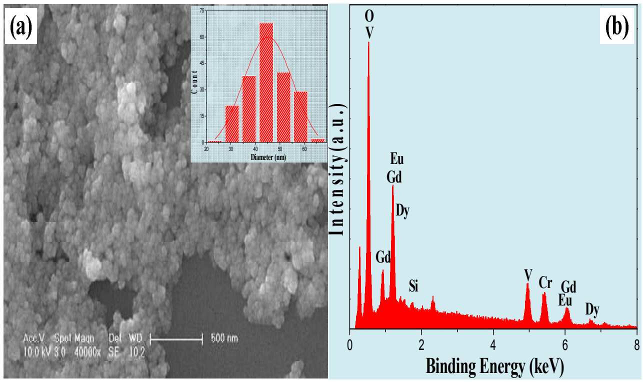

Fig. 2 (a) FE-SEM image and (b) EDS spectrum of $GdVO_4$: $0.02Dy^{3+}$, $0.02Eu^{3+}$ samples. Inset of (a) is the particle size distribution.

3.2 Luminescence properties

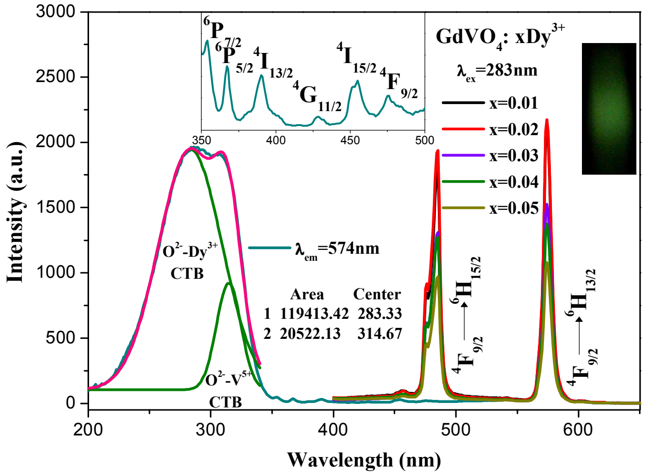

Fig. 3 PL excitation spectrum (left) for $GdVO_4$: $0.02Dy^{3+}$ and emission (right) spectra for $GdVO_4$: xDy^{3+} (x=0.01-0.05) samples. Insets are enlarged excitation spectrum for $GdVO_4$: $0.02Dy^{3+}$ at the range of 350 to 500 nm and luminescent photograph of $GdVO_4$: $0.02Dy^{3+}$ under 283 nm illumination, respectively.

Fig. 3 presents the excitation and emission spectra for Dy^{3+} singly activated $GdVO_4$ samples and their corresponding luminescent photograph under the excitation of a 283 nm UV-lamp. The excitation spectrum was obtained by monitoring the characteristic emission of Dy^{3+} (574 nm, $^4F_{9/2}\rightarrow{}^6H_{13/2}$). It can be found that the excitation spectrum shows a broad excitation band consisting of two peaks by dealing with Gaussian fitting: the former centered at 283 nm corresponds to the CTB for O^{2-}-Dy^{3+} from oxygen 2p excited state to Dy^{3+} 4f state and the other centered at 314 nm corresponds to O^{2-}-V^{5+} charge transfer transition from oxygen 2p states to the empty d states of central vanadium atom in the VO_4^{3-} group, indicating CTB and host can effectively transfer energy to Dy^{3+} ions[27,30]. In addition, many sharp peaks in the longer wavelength region from 350 to 500 nm can be observed. These peaks at 354, 367, 390, 429, 455 and 475 nm can be assigned to f-f transitions of Dy^{3+} from the ground state $^6H_{15/2}$ to higher excited states $^6P_{7/2}$, $^6P_{5/2}$, $^4I_{13/2}$, $^4G_{11/2}$, $^4I_{15/2}$ and $^4F_{9/2}$, respectively. Upon excitation at 283 nm, the as-prepared $GdVO_4$: xDy^{3+} samples exhibit blue and yellow emissions which due to transitions from $^4F_{9/2}$ to $^6H_{15/2}$ and $^6H_{13/2}$, suggesting multicolor emissions can be realized by co-doping Dy^{3+} and the other appropriate luminescence rare earth ions. Moreover, the emission intensity of Dy^{3+} ions increases until the Dy^{3+} concentration is above 0.02 and then decreases for the concentration quenching effect, which ascribed to the cross relaxation between neighboring Dy^{3+} ions at a high concentration: Dy^{3+} ($^4F_{9/2}$) + Dy^{3+} ($^6H_{15/2}$) → Dy^{3+} ($^6F_{3/2}$) + Dy^{3+} ($^6F_{11/2}$)[31]. As the concentration of Dy^{3+} ions increases, the distance between Dy^{3+} ions will become small enough to allow a resonant energy transfer to occur. The electrons at higher energy level of $^4F_{9/2}$ are quenched through getting back to the lower energy level of $^6F_{3/2}$ and giving the released energy to the electrons at ground state $^6H_{15/2}$, which lead to the electron transitions from ground state $^6H_{15/2}$ to the higher energy level of $^6H_{11/2}$[31]. It can be seen that the as-prepared $GdVO_4$ crystals doped with Dy^{3+} show green emission under UV irradiation, as shown in the inset of Fig. 3.

Fig. 4 shows excitation and emission spectra of the as-prepared $GdVO_4$: $0.02Eu^{3+}$ samples and their corresponding luminescent photograph upon 283 nm excitation. The excitation spectrum monitored the emission of Eu^{3+} $^5D_0\rightarrow{}^7F_2$ transition at 620 nm contains a strong broad band absorption from 200 to 350 nm caused by the O^{2-}-Eu^{3+} CTB and O^{2-}-V^{5+} charge transfer transition[27,30], and O^{2-}-V^{5+} charge transfer transition corresponds to the transitions from the $^1A_2(^1T_1)$ ground state to $^1A_1(^1E)$ and $^1E(^1T_2)$ excited state of VO_4^{3-} group in the view of molecular orbital theory[26]. The existence of O^{2-}-Eu^{3+} CTB and O^{2-}-V^{5+} charge transfer transition indicates energy transfer from CTB and VO_4^{3-} group to Eu^{3+} ions is efficient and Eu^{3+} ions could be effectively excited via energy transfer from CTB and VO_4^{3-} group to the Eu^{3+} ions in the Eu^{3+} ions activated $GdVO_4$ samples. Furthermore, there are several sharp peaks in the longer wavelength region at 363, 377, 384, 396, 418 and 467 nm originated from f-f transitions within the $4f^6$ configuration of the Eu^{3+} ions from the $^7F_0$ ground state to the $^5D_4$, $^5G_3$, $^5L_7$, $^5L_6$, $^5D_3$, and $^5D_2$ excited states, respectively. The emission spectrum of $GdVO_4$: $0.02Eu^{3+}$ was obtained via exciting with 283 nm. One can see that there are a number of emission peaks in the range 500-750 nm at 537, 559, 595, 616, 620, 651 and 699 nm, which correspond to $^5D_1\rightarrow{}^7F_1$, $^5D_1\rightarrow{}^7F_0$, $^5D_0\rightarrow{}^7F_1$, $^5D_0\rightarrow{}^7F_2$, $^5D_0\rightarrow{}^7F_3$ and $^5D_0\rightarrow{}^7F_4$ transitions, respectively. The results indicate that the CTB and VO_4^{3-} group can absorb an excitation wavelength of 283 nm and efficiently transfer the energy to the Eu^{3+} activators. It can be seen clearly that the emission spectrum is dominated by the transition at 620 nm derived from the Eu^{3+} $^5D_0\rightarrow{}^7F_2$ electric dipole transition, implying that Eu^{3+} occupy the site without inversion symmetry in the $GdVO_4$ host.

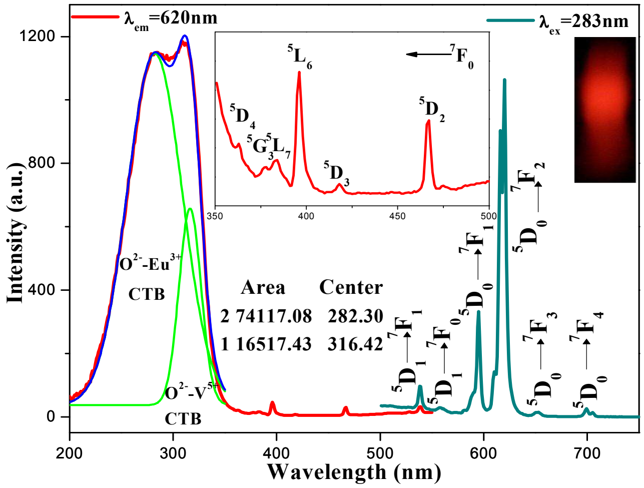

Fig. 4 PL excitation and emission spectra for $GdVO_4$: $0.02Eu^{3+}$ samples. Insets are amplificatory excitation spectrum for $GdVO_4$: $0.02Eu^{3+}$ at the range of 350 to 500 nm and luminescent photograph of $GdVO_4$: $0.02Eu^{3+}$ under 283 nm illumination, respectively.

Fig. 5 shows the excitation spectra for $GdVO_4$: $0.02Dy^{3+}$, xEu^{3+} (x=0-0.05) samples with monitoring 574 nm (a) and 620 nm (b), respectively. When monitoring by the emission of Dy^{3+} (574 nm, $^4F_{9/2}$-$^6H_{13/2}$) and Eu^{3+} (620 nm, $^5D_0$-$^7F_2$), the excitation spectra are similar to that of $GdVO_4$: Dy^{3+} and $GdVO_4$: Eu^{3+}. The absorption intensity of CTB and VO_4^{3-} group decreases gradually with increasing the content of Eu^{3+} ions in Fig. 5 (a) while increases first until the Eu^{3+} concentration is above 0.03 then decreases in Fig. 5 (b). The intense absorptions of CTB and VO_4^{3-} group strongly suggest that the energy transfer from VO_4^{3-} group and CTB to Dy^{3+} and Eu^{3+} ions is efficient.

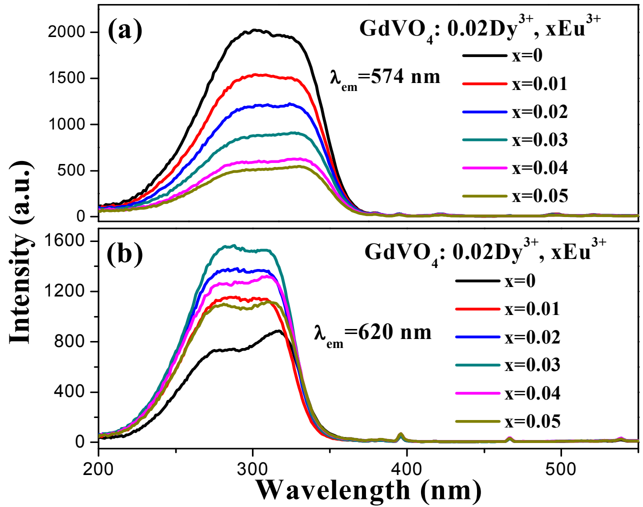

Fig. 5 Excitation spectra of $GdVO_4$: $0.02Dy^{3+}$, xEu^{3+} (x=0-0.05) samples monitored by (a) 574 nm and (b) 620 nm, respectively.

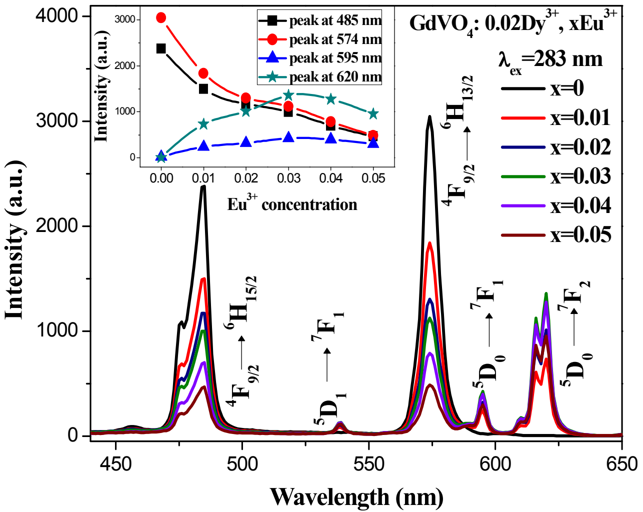

Fig. 6 PL emission spectra of the $GdVO_4$: $0.02Dy^{3+}$, xEu^{3+} (x=0.01-0.06) samples (λ_{ex}=283 nm), and the inset is the relative intensity of the Dy^{3+} and Eu^{3+} emissions as a function of the Eu^{3+} concentration.

In order to investigate the luminescent characteristics both of Dy^{3+} and Eu^{3+} in $GdVO_4$, a series of Dy^{3+} and Eu^{3+} co-doped samples with fixed Dy^{3+} content at 0.02 and varied Eu^{3+} concentration from 0.01 to 0.06 were prepared. Fig. 6 presents the emission spectra for the as-prepared samples upon the excitation at 283 nm. One can see that the typical emissions for both Dy^{3+} and Eu^{3+} ions can be observed. In addition, the emission intensity of Dy^{3+} ions is found to decrease monotonously with increasing the Eu^{3+} content. However, the emission intensity of Eu^{3+} increases gradually until the content of Eu^{3+} is above 0.03 then decrease because of the concentration quenching effect: Eu^{3+} ($^5D_1$) + Eu^{3+} ($^7F_0$) → Eu^{3+} ($^5D_0$) + Eu^{3+} ($^7F_3$)[31], which takes place between the two neighboring Eu^{3+} ions at a high concentration. The cross relaxation from $^5D_1$ to $^5D_0$ occurs originated from the interaction between Eu^{3+} ions, which enhances the transitions from $^5D_0$ to ^7F_J with a red emission[31]. The results indicate that multicolor photoluminescence can be achieved by varying the concentration of Dy^{3+} and Eu^{3+} ions.

To further confirm the conclusion derived from Fig. 6 that multicolor emissions can be gained by adjusting the content of Dy^{3+} and Eu^{3+} ions, a series of $GdVO_4$: $0.02Eu^{3+}$, xDy^{3+} (x=0.01-0.05) samples were synthesized. The emission spectra for the samples have been exhibited in Fig. 7. It is noted that the emission intensity of Eu^{3+} monotonously decreases although the Eu^{3+} content is fixed. Furthermore, the emission intensity of Dy^{3+} increases at first and then decreases when the concentration of Dy^{3+} is above 0.03 because of the concentration quenching effect. The conclusions further support the results that multicolor luminescence can be realized by modulating the content of Dy^{3+} and Eu^{3+} ions when excited by a single excitation wavelength.

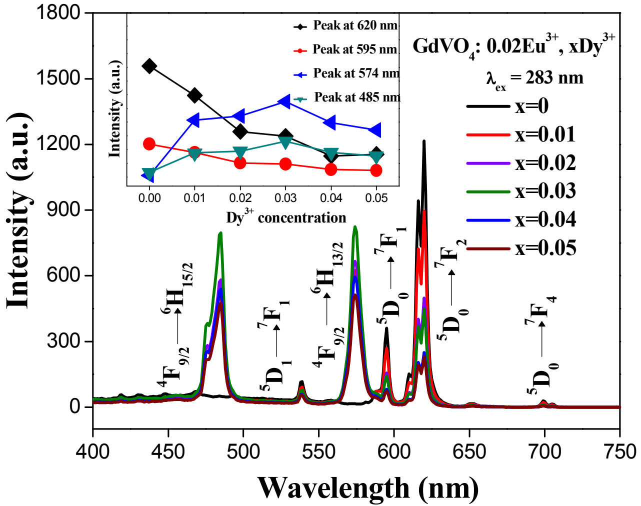

Fig. 7 PL emission spectra of the $GdVO_4$: $0.02Eu^{3+}$, xDy^{3+} (x=0.01-0.05) samples (λ_{ex}=283 nm), and the inset is the relative intensity of the Dy^{3+} and Eu^{3+} emissions as a function of the Dy^{3+} concentration.

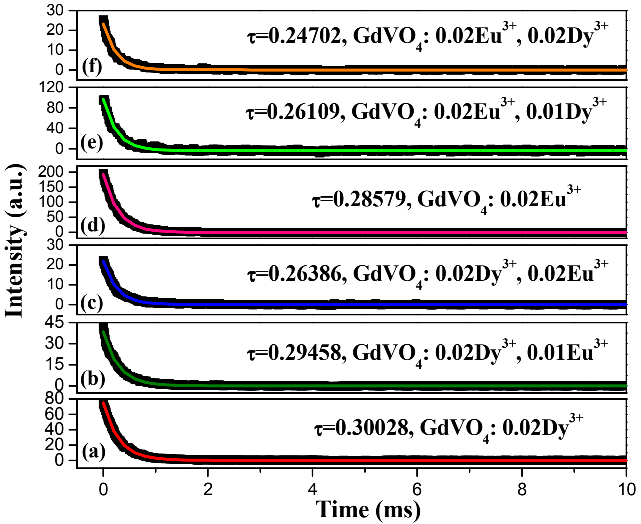

Fig. 8 Decay curves for the luminescence of Dy^{3+} ions in the $GdVO_4$: $0.02Dy^{3+}$, xEu^{3+}(x=0-0.02) system corresponding to the curves (a)-(c) and Eu^{3+} ions in the $GdVO_4$: $0.02Eu^{3+}$, yDy^{3+}(x=0-0.02) system corresponding to the curves (d)-(f).

To further understand the excitation and de-excitation process in depth, the lifetime of transitions for Dy^{3+} or/and Eu^{3+} ions doped $GdVO_4$ system was investigated. Fig. 8 (a)-(c) exhibit the decay curves for the luminescence of Dy^{3+} ions in the $GdVO_4$: $0.02Dy^{3+}$, xEu^{3+}(x=0-0.02) system with excited at 283 nm and monitored at 574 nm. The decay curves for the luminescence of Eu^{3+} ions in the $GdVO_4$: $0.02Eu^{3+}$, yDy^{3+}(x=0-0.02) system with excited at 283 nm and monitored at 620 nm have been presented in Fig. 8 (d)-(e). All of the curves can be well fitted with a single exponential function of $I=I_0+A\exp(-x/\tau)$ (τ corresponds to the lifetime of Dy^{3+} or Eu^{3+} ions)[20]. The lifetime of Dy^{3+} ions decreases gradually with the content of Eu^{3+} ions increasing, indicating Dy^{3+} ions stay in excited state with less time. The occasion for Eu^{3+} ions is similar to Dy^{3+} ions.

It is well accepted that multicolor luminescence also can be achieved by adopting different excitation wavelengths. Fig. 9 shows emission spectra of $GdVO_4$: $0.02Dy^{3+}$, $0.04Eu^{3+}$ sample under different wavelengths excitation. One can see that the sample exhibit the typical emissions of both Dy^{3+} and Eu^{3+} under 283, 305 and 354 nm excitation. Upon excitation with 390 and 455 nm, one can see that the intense emissions of Dy^{3+} and weak emissions of Eu^{3+}. However, one can mainly see the characteristic emissions of Eu^{3+} under excitation at 396 and 467 nm. The results powerfully imply the multicolor luminescence can be achieved in $GdVO_4$ system by adopting the appropriate excitation wavelength.

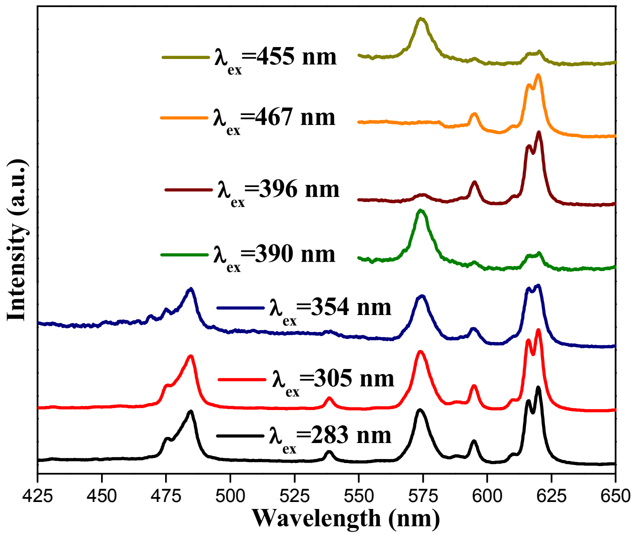

Fig. 9 PL emission spectra of $GdVO_4$: $0.02Dy^{3+}$, $0.04Eu^{3+}$ samples under different wavelengths excitation.

In view of all the photoluminescence properties, Fig. 10 exhibits the proposed scheme of energetic processes occurring in the $GdVO_4$: Dy^{3+}, Eu^{3+} samples. Based on the above discussions, both of O-Dy^{3+}/Eu^{3+} CTB and VO_4^{3-} group make contributions to the emissions of Dy^{3+} and Eu^{3+}. During the whole excitation procedure, electronic transitions from the O2p valence to the Dy/Eu (5d6s) conduction band occur under UV light irradiation and then the electrons get back to the lower energy levels once again through blue emission as well as transfer energy to Dy^{3+} and Eu^{3+} ions, the other energy is released through cross relaxation. Also, the transitions from $^1A_2$ ($^1T_1$) ground state of VO_4^{3-} group to $^1A_1$ (^1E) and ^1E ($^1T_2$) excited states take place and VO_4^{3-} group transfer energy to Dy^{3+} and Eu^{3+} ions in de-excitation process.

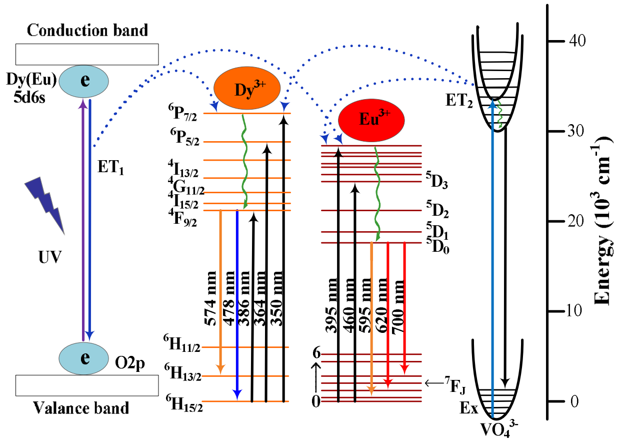

Fig. 10 The proposed scheme of energetic processes occurring in the $GdVO_4$: Dy^{3+}, Eu^{3+} samples.

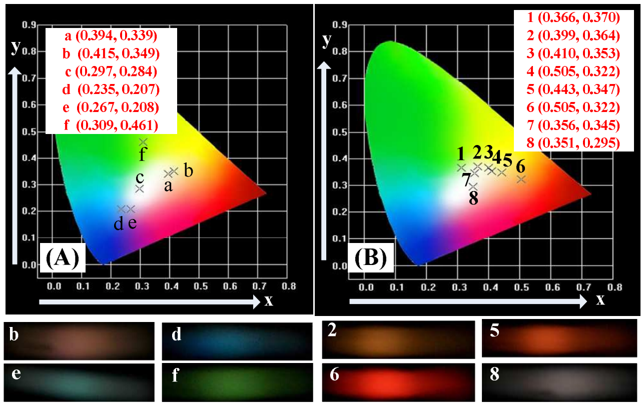

Fig. 11 (A) CIE chromaticity diagram of $GdVO_4$: $0.02Dy^{3+}$, $0.04Eu^{3+}$ phosphors under 283 nm (a), 305 nm (b) 354 nm (c), 390 nm (d), 396 nm (e), and 467 nm (f) excitation; (B) CIE chromaticity diagram of $GdVO_4$: $0.02Eu^{3+}$, xDy^{3+} (x=0, 0.03, 0.05) phosphors corresponding to the points of 6-8 and $GdVO_4$: $0.02Dy^{3+}$, xEu^{3+} (x=0, 0.01, 0.02, 0.03, 0.06) phosphors corresponding to the points of 1-5 upon 283 nm excitation, and the selected luminescence photographs of the corresponding samples.

Fig. 11 shows the CIE chromaticity diagram and corresponding selected luminescence photographs of $GdVO_4$: $0.02Dy^{3+}$, $0.04Eu^{3+}$ under different excitation wavelengths and Dy^{3+} or/and Eu^{3+} doped $GdVO_4$ as a function of Dy^{3+} or Eu^{3+} content excited at 283 nm. From Fig. 11 (A), one can see that $GdVO_4$: $0.02Dy^{3+}$, $0.04Eu^{3+}$ sample shows different emission color under different wavelengths illumination. The CIE chromaticity coordinates were discovered to be (a, 0.394, 0.339), (b, 0.415, 0.349), (c, 0.297, 0.284), (d, 0.235, 0.207), (e, 0.267, 0.208) and (f, 0.309, 0.461) when excited by 283, 305, 354, 390, 396 and 467 nm, respectively. Moreover, it also can be found that the emission color can be tuned through varying the Dy^{3+} or Eu^{3+} content although using a single wavelength as pumping source. From Fig.11(B), the corresponding CIE chromaticity coordinates were calculated to be (1, 0.313, 0.365), (2, 0.366, 0.370), (3, 0.399, 0.364), (4, 0.410, 0.353), (5, 0.443, 0.347) for $GdVO_4$: $0.02Dy^{3+}$, xEu^{3+} (x=0, 0.01, 0.02, 0.03, 0.06) and (6, 0.505, 0.322), (7, 0.356, 0.345), (8, 0.351, 0.295) for $GdVO_4$: $0.02Eu^{3+}$, xDy^{3+} (x=0, 0.03, 0.05). All of the results indicate that multicolor luminescence can be achieved through adopting different excitation wavelengths or adjusting appropriate concentration of Dy^{3+} and Eu^{3+} in $GdVO_4$ system.

3.3 Magnetic properties

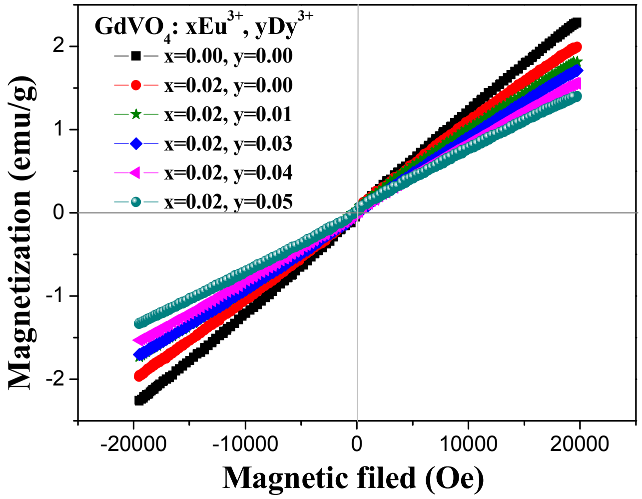

Fig. 12 Magnetization as a function of applied magnetic field for $GdVO_4$: xEu^{3+}, yDy^{3+} (x=0, 0.02; y=0-0.05) samples, respectively.

The as-prepared samples not only exhibit excellent fluorescent properties but also magnetic properties because Gd^{3+} ions possess seven unpaired electrons which could efficiently alter the relaxation time of surrounding water protons[17]. Generally speaking, Gd-based inorganic compounds exhibit paramagnetic properties because Gd atom possesses a permanent magnetic moment ascribed from the unpaired electrons. The seven unpaired inner 4f electrons of Gd^{3+} ions are closely bound to the nucleus and can be effectively shield by the outer closed-shell $5s^25p^6$ electrons from the crystal field, which gives rise to the magnetic properties of Gd^{3+} ions. The magnetic moments related to Gd^{3+} ions are all localized and non-interacting, which led to paramagnetism of Gd^{3+} ions[32,33]. The magnetic properties of the as-prepared samples were analyzed by a VSM. Fig. 12 shows the magnetization for $GdVO_4$: xEu^{3+}, yDy^{3+} (x=0, 0.02; y=0-0.05) samples with varying the applied field at room temperature. From the nature of the curve, it is clear that all the samples are found to exhibit paramagnetic properties and the magnetization can reach 2.29022, 1.99375, 1.81388, 1.71031, 1.54959 and 1.40032 emu/g when the applied magnetic field is 20 kOe for $GdVO_4$: xEu^{3+}, yDy^{3+} (x=0, 0.02; y=0-0.05) samples, respectively. It is worth noting that the magnetization of the samples changes at 20 kOe because Gd^{3+} ions are substituted by Dy^{3+} or/and Eu^{3+} ions. The magnetization of the samples decreases in sequence with increasing the contents of Dy^{3+} and Eu^{3+} ions for the deficiency of Gd^{3+} ions. The results suggest that this style of materials has great potential applications in the field of biomedical science[34-36].

4 Conclusions

In summary, a series of color-tunable $GdVO_4$: Dy^{3+}, Eu^{3+} nanoparticles with an average diameter of about 45 nm were successfully obtained via a hydrothermal method at 180 °C for 24 h. The intense characteristic blue and yellow emissions of Dy^{3+} and red emission of Eu^{3+} can be observed because the CTB and VO_4^{3-} group can efficiently absorb UV light and transfer the energy to Dy^{3+} or Eu^{3+} ions. By adopting different excitation wavelengths or adjusting appropriate concentration of Dy^{3+} and Eu^{3+} ions, tunable photoluminescence are realized in Dy^{3+} and Eu^{3+} doped $GdVO_4$ system. The as-obtained samples exhibit paramagnetic properties at room temperature and the magnetization of the samples decreases when Gd^{3+} ions are replaced by Dy^{3+} and Eu^{3+} ions at 20 kOe. The results imply that the as-prepared samples can be applied in the fields of biomedical science and full-color display.

Acknowledgements

This work was financially supported by the National Natural Science Foundation of P.R. China (NSFC) (Grant No. 51072026, 50972020) and the Development of Science and Technology Plan Projects of Jilin Province (Grant No. 20130206002GX).

Notes and references

Key Laboratory of Applied Chemistry and Nanotechnology at Universities of Jilin Province, Changchun University of Science and Technology, Changchun, China. Fax: +86-431-85383815; Tel: +86-431-85582574; E-mail: liuguixia22@163.com

1. H. Hu, D. Li, S. Liu, M. Wang, R. Moats, P. S. Conti and Z. Li, *Biomaterials*, **2014**, *35*, 8649-8658.
2. X. He, L. Zhang, G. Chen and Y. Hang, *J. Alloys Compd.*, **2009**, *467*, 366-369.
3. Y. Yan, J. Wang, M. Hojamberdiev, Z. Lu, B. Ren and Y. Xu, *J. Alloys Compd.*, **2014**, *597*, 282-290.
4. Z. Xu, B. Feng, Y. Gao, Q. Zhao, D. Sun, X. Gao, K. Li, F. Ding and Y. Sun, *CrystEngComm*, **2012**, *14*, 5530-5538.
5. W. Yin, L. Zhou, Z. Gu, G. Tian, S. Jin, L. Yan, X. Liu, G. Xing, W. Ren, F. Liu, Z. Pan and Y. Zhao, *J. Mater. Chem.*, **2012**, *22*, 6974-6981.
6. L. Yang, G. Li, M. Zhao, J. Zheng, D. Luo, Y. Zheng and L. Li, *Eur. J. Inorg. Chem.*, **2013**, *2013*, 5999-6008.
7. X. Kang, D. Yang, Y. Dai, M. Shang, Z. Cheng, X. Zhang, H. Lian, P. a. Ma and J. Lin, *Nanoscale*, **2013**, *5*, 253-261.
8. S. Huang, Z. Cheng, P. a. Ma, X. Kang, Y. Dai and J. Lin, *Dalton Trans.*, **2013**, *42*, 6523-6530.
9. T. Kim, N. Lee, Y. I. Park, J. Kim, J. Kim, E. Y. Lee, M. Yi, B.-G. Kim, T. Hyeon, T. Yu and H. B. Na, *RSC Adv.*, **2014**, *4*, 45687-45695.
10. K. Dong, E. Ju, J. Liu, X. Han, J. Ren and X. Qu, *Nanoscale*, **2014**, *6*, 12042-12049.
11. S. Som, P. Mitra, V. Kumar, V. Kumar, J. J. Terblans, H. C. Swart and S. K. Sharma, *Dalton Trans.*, **2014**, *43*, 9860-9871.
12. Y. Zhou, J. Xu, Z. Zhang and M. You, *J. Alloys Compd.*, **2014**, *615*, 624-628.
13. Y. I. Jeon, L. Krishna Bharat and J. S. Yu, *J. Alloys Compd.*, **2015**, *620*, 263-268.
14. Y. Deng, S. Yi, J. Huang, J. Xian and W. Zhao, *Mater. Res. Bull.*, **2014**, *57*, 85-90.
15. V. R. Bandi, B. K. Grandhe, H.-J. Woo, K. Jang, D.-S. Shin, S.-S. Yi and J.-H. Jeong, *J. Alloys Compd.*, **2012**, *538*, 85-90.
16. Y. Yan, M. Hojamberdiev, Y. Xu, J. Wang and Z. Luan, *Mater. Chem. Phys.*, **2013**, *139*, 298-304.
17. X. Kang, D. Yang, P. a. Ma, Y. Dai, M. Shang, D. Geng, Z. Cheng and J. Lin, *Langmuir*, **2013**, *29*, 1286-1294.
18. N. Shanta Singh, R. S. Ningthoujam, G. Phaomei, S. D. Singh, A. Vinu and R. K. Vatsa, *Dalton Trans.*, **2012**, *41*, 4404-4412.
19. H. Guan, G. Liu, J. Wang, X. Dong and W. Yu, *New J. Chem.*, **2014**, *38*, 4901-4907.
20. H. Guan, G. Liu, J. Wang, X. Dong and W. Yu, *Dalton Trans.*, **2014**, *43*, 10801-10808.
21. R. Krishnan and J. Thirumalai, *New J. Chem.*, **2014**, *38*, 3480-3491.
22. J. Cho and C. H. Kim, *RSC Adv.*, **2014**, *4*, 31385-31392.

23. Y. Liu, G. Liu, J. Wang, X. Dong and W. Yu, *Inorg. Chem.*, **2014**, *53*, 11457-11466.
24. W. B. Dai, S. Ye, E. L. Li, P. Z. Zhuo and Q. Y. Zhang, *J. Mater. Chem. C*, **2015**.
25. S. Tang, M. Huang, J. Wang, F. Yu, G. Shang and J. Wu, *J. Alloys Compd.*, **2012**, *513*, 474-480.
26. N. S. Singh, R. S. Ningthoujam, N. Yaiphaba, S. D. Singh and R. K. Vatsa, *J. Appl. Phys.*, **2009**, *105*, 064303.
27. A. Szczeszak, T. Grzyb, Z. Śniadecki, N. Andrzejewska, S. Lis, M. Matczak, G. Nowaczyk, S. Jurga and B. Idzikowski, *Inorg. Chem.*, **2014**, *53*, 12243-12252.
28. L. Yang, L. Li, M. Zhao and G. Li, *Phys. Chem. Chem. Phys.*, **2012**, *14*, 9956-9965.
29. B. Shao, Q. Zhao, N. Guo, Y. Jia, W. Lv, M. Jiao, W. Lu and H. You, *CrystEngComm*, **2014**, *16*, 152-158.
30. Y. Liu, G. Liu, X. Dong, J. Wang and W. Yu, *RSC Adv.*, **2014**, *4*, 58708-58716.
31. M. Shang, D. Geng, X. Kang, D. Yang, Y. Zhang and J. Lin, *Inorg. Chem.*, **2012**, *51*, 11106-11116.
32. F. He, N. Niu, L. Wang, J. Xu, Y. Wang, G. Yang, S. Gai and P. Yang, *Dalton Trans.*, **2013**, *42*, 10019-10028.
33. Z. Xu, C. Li, D. Yang, W. Wang, X. Kang, M. Shang and J. Lin, *Phys. Chem. Chem. Phys.*, **2010**, *12*, 11315-11324.
34. N. O. Nunez, S. Rivera, D. Alcantara, J. M. de la Fuente, J. Garcia-Sevillano and M. Ocana, *Dalton Trans.*, **2013**, *42*, 10725-10734.
35. J. Shen, L.-D. Sun and C.-H. Yan, *Dalton Trans.*, **2008**, 5687-5697.
36. D. Yang, P. a. Ma, Z. Hou, Z. Cheng, C. Li and J. Lin, *Chem. Soc. Rev.*, **2015**, *44*, 1416-1448.